

Violet Electroluminescence of AlInGaN–InGaN Multiquantum-Well Light-Emitting Diodes: Quantum-Confined Stark Effect and Heating Effect

Jun Li, S. L. Shi, Y. J. Wang, S. J. Xu, D. G. Zhao, J. J. Zhu, H. Yang, and F. Lu

Abstract—Electroluminescence (EL) from AlInGaN–InGaN multiquantum-well violet light-emitting diodes is investigated as a function of forward bias. Two distinct regimes have been identified: 1) quantum-confined Stark effect at low and moderately high forward biases; 2) heating effect at high biases. In the different regimes, the low-temperature EL spectra exhibit different spectral features which are discussed in detail.

Index Terms—AlInGaN, electroluminescence (EL), InGaN, light-emitting diodes (LEDs), multiple quantum wells (QWs).

SUCCESSFUL demonstration and commercialization of III nitrides-based light-emitting devices including laser diodes (LDs) might be one of the biggest technology breakthroughs in the past decade due to their tremendous application value [1]. Usually, strained GaN–InGaN quantum wells (QWs) act as the light-emitting active layer in this new class of light-emitting diodes (LEDs) and LDs. When many studies have been continuously devoted to increase understanding of fundamental physical mechanisms of GaN–InGaN QWs [2]–[7], AlInGaN–InGaN QWs have attracted an increasing interest due to the ability for emission wavelength and lattice mismatch engineering [8]–[12]. To date, the knowledge of optical properties of AlInGaN–InGaN QWs is quite limited partially due to the difficult growth of these heterostructures with device quality.

In this letter, we present a study on the electroluminescence (EL) of AlInGaN–InGaN QW LEDs emitting violet light. The spectral evidence for the quantum-confined Stark effect (QCSE) and heating effect has been observed.

The sample used in the present study was grown on sapphire by low-pressure metal–organic vapor phase epitaxy. During

the growth of the sample, ammonia (NH₃), trimethylaluminum (TMAI), trimethylgallium (TMGa), and trimethylindium (TMIn) were used as N, Al, Ga, and In precursors, respectively. High pure hydrogen gas was used as the carrier gas. Following a 3- μm -thick n⁺-GaN (Si: $5 \times 10^{18} \text{ cm}^{-3}$) bottom contact layer, three periods of undoped AlInGaN–InGaN QWs with 28-nm-thick barrier layers and 2-nm-thick well layers were grown. Then the top contact layer of 200-nm-thick p-GaN (Mg: $3 \times 10^{17} \text{ cm}^{-3}$) was grown. During the growth of AlInGaN barrier layers, the molar flows of TMAI, TMIn, and TMGa were controlled at 2.5, 22.7, and 9.47 $\mu\text{mol}/\text{min}$, respectively. For the growth of InGaN well layers, molar flows of TMIn and TMGa were 87.5 and 5.12 $\mu\text{mol}/\text{min}$, respectively. Under these conditions, the elemental compositions of barrier layers and well layers are Al_{0.075}In_{0.045}Ga_{0.88}N and In_{0.08}Ga_{0.92}N, respectively. The sample was finally processed into mesa device structures. For the low-temperature EL measurements, the diode was mounted on the sample holder of a liquid nitrogen Dewar. An Acton SP307 monochromator equipped with a 1200-grooves/mm grating was employed to disperse the EL signal from the top of diode and a Hamamatsu R928 PMT was used to detect the dispersed signal. Variable-temperature current–voltage (*I*–*V*) curves of the diode, which was mounted on the cold finger of a Janis closed-cycle cryostat, were measured by using Keithley source meter.

First, EL spectra (thin solid lines) of the device were measured at room temperature as a function of forward bias as shown in Fig. 1. The turn-on voltage of the diode is about 2.70 V at room temperature. The spectra show oscillatory fine structures which are frequently observed in the emission spectra of InGaN-based LEDs due to the Fabry–Pérot interference effect [1], [13]. The period of oscillatory structures is about 5 nm. In order to analyze the spectral parameters such as peak position, integrated intensity, and full-width at half-maximum (FWHM) height of the EL spectra, the EL spectra were simply averaged and the resulting curves were shown as thick solid lines in the figure. Unlike the observation in some GaN–InGaN QW LEDs [13], [14], the peak position of EL spectra of AlInGaN–InGaN QW LED does not exhibit a clear blues shift with the forward bias (hence injection current) at room temperature. Conversely, red shift of the peak position begins accompanying with the evident broadening of the lineshape for the forward bias higher than 3.75 V. In particular, the peak position red shifts faster when the bias is beyond 4.90 V. At the same time, the EL intensity starts to drop. All these behaviors can be consistently explained by the heating effect of the device, which is evidenced by the low-temperature EL and variable-temperature *I*–*V* data discussed below.

Manuscript received September 22, 2006; revised February 24, 2007. This work was supported in part by the Hong Kong RGC-CERG under Grant HKU 7036/03P.

J. Li is with the Department of Physics, Fudan University, Shanghai 200433, China, and also with the Department of Physics, The University of Hong Kong, Hong Kong SAR, China.

S. L. Shi and S. J. Xu are with the Department of Physics, The University of Hong Kong, Hong Kong SAR, China (e-mail: sjxu@hkucc.hku.hk).

Y. J. Wang was with the Department of Physics, The University of Hong Kong, Hong Kong SAR, China. She is now with the Clarendon Laboratory, Oxford OX1 3PU, U.K.

D. G. Zhao, J. J. Zhu, and H. Yang are with the State Key Laboratory on Integrated Optoelectronics, Institute of Semiconductors, Chinese Academy of Sciences, Beijing 100083, China.

F. Lu is with the Department of Physics, Fudan University, Shanghai 200433, China.

Color versions of one or more of the figures in this letter are available online at <http://ieeexplore.ieee.org>.

Digital Object Identifier 10.1109/LPT.2007.896575

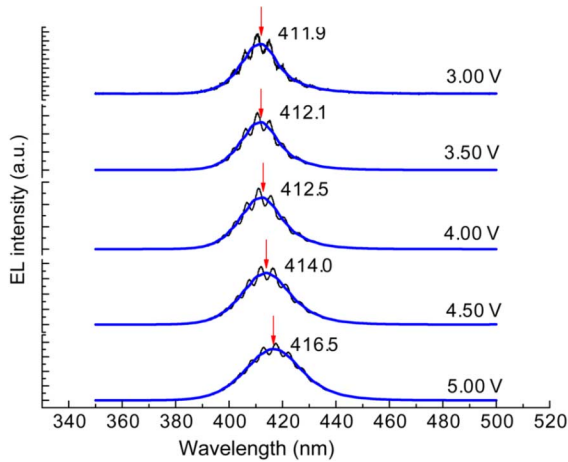


Fig. 1. Representative room-temperature EL spectra (thin solid lines) of the device at different forward biases. The influence of interference fringes due to the Fabry-Pérot effect can be efficiently eliminated through conducting average to the experimental spectra, as indicated by thick solid lines in the figure. The peak position is indicated by a vertical arrow.

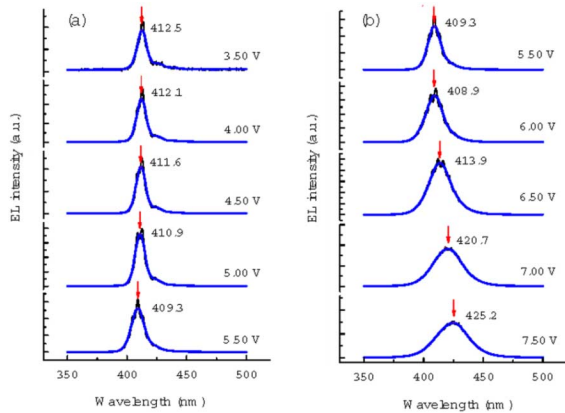


Fig. 2. Representative 77 K EL spectra (thin solid lines) of the device at different forward biases. Averaging curves (thick solid lines) of the experimental spectra are also given for eliminating the influence of interference fringes due to the Fabry-Pérot effect. The peak position is indicated by a vertical arrow.

Fig. 2 shows the EL spectra of the device at 77 K under different forward biases. The spectral parameters extracted from the spectra were shown in Fig. 3. Clearly, blue shift of the EL peak takes place with increasing the forward bias lower than 5.60 V. However, when the bias is higher than 6.0 V, the EL red shifts rapidly. A more careful look at the spectral parameters' evolution with the forward bias tells us that the three different evolution regions can be resolved: 1) the slow blue-shift region for the low biases below 5.20 V, i.e., the peak position blue shifts from 3.006 eV at 3.50 V to 3.019 eV at 5.20 V, accompanying with linear increase of the emission intensity and almost unchanged FWHM; 2) the fast blue-shift region for the moderately high biases from 5.20 to 5.60 V, for example, the blue-shift amount is as much as about 18 meV in this bias range, and both intensity and FWHM increase quite rapidly; 3) the red shift region for the high biases beyond 6.0 V, simultaneously, the emission intensity starts to decrease while the FWHM continuously increases.

The blue shift of the EL peak position with the forward bias can be well understood in terms of the QCSE effect discovered

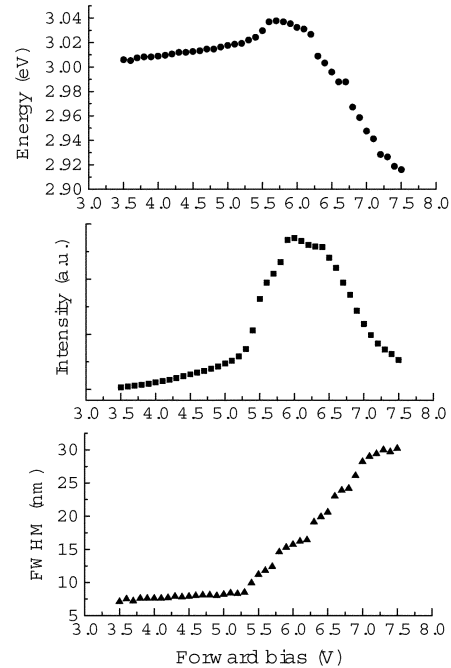


Fig. 3. Peak positions (solid circles), integrated intensity (solid squares), and FWHM (solid up triangles) extracted from the 77 K EL spectra.

by Miller *et al.* [15]. The QCSE effect manifests in a red shift of the energy of excitons confined in quantum structures under action of external or internal perpendicular electric field. It is well known that the lattice mismatch strain usually exists in the InGa_N-based QWs including AlInGa_N-InGa_N QWs [11], [16]. Due to the piezoelectric nature of the InGa_N alloy, the mismatch strain can introduce a huge electrical field in the well regions. Another origin causing the built-in electric field in the active region is due to the P-N junction effect of the p-i-n structured LED diode. When the carriers are electrically or optically injected into the InGa_N well regions, this built-in electric field could be effectively screened out by the carriers. As a result, a blue shift of the exciton energy and thus photonic energy of the excitonic absorption or emission should take place [16], [17]. For the AlInGa_N-InGa_N QW LEDs under study, the observed slow blue shift of EL peak in the low bias region can be attributed to the screening of the built-in electric field by the electrically injected carriers. Such an attribution is supported by the *I-V* characteristics of the diode shown in Fig. 4. At 77 K, the injection current of the diode steadily grows as the forward bias increases below 5.20 V.

When the forward bias becomes moderately high, the injection current and, hence, carrier concentration rapidly increases. The injection of high density of carriers can lead to the presence of band-filling effect. The spectral features for the band-filling effect include the significant increase of the EL intensity at higher energy side and noticeable shift of the EL peak towards the higher energy side [5], [13], [18], as observed in Fig. 3. It is worth mentioning that the bandgap renormalization could occur when the high density of carriers sustain in the InGa_N active layers [5]. The bandgap renormalization tends to narrow the bandgap. For the case studied here, it is difficult to distinguish the bandgap renormalization from the heating effect that will be discussed below.

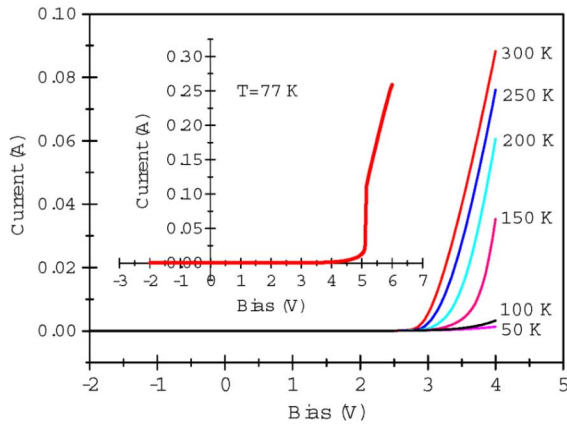


Fig. 4. I – V characteristics of the diode at different temperatures. The inset shows I – V curve of the diode measured at 77 K.

Under high forward bias, i.e., higher than 6.0 V, the injection current and thus carrier density becomes very large. Under such conditions, nonradiative recombination of a large number of carriers will make the device hot quickly. Increase of lattice temperature will result in shrinking of the material bandgap and broadening of the emission peak due to phonon scattering [19]. That is why the EL peak rapidly red shifts and the intensity drops at 77 K under the condition of large injection current. At room temperature, the situation becomes more serious. On one hand, due to the thermal activation of more nonradiative centers and increase of phonon-assisted nonradiative recombination, the nonradiative recombination rate of carriers in semiconductors at room temperature is usually larger than at low temperature. In other words, LEDs are much easier to become hot at room temperature and under the same carrier injection. On the other hand, the injection current of the diode is a strong function of temperature as shown in Fig. 4. For example, the injection current of the diode at 300 K under 4.0 V is comparable with that at 77 K under 5.1 V. Therefore, both the large injection current and nonradiative recombination rate of the diode at room temperature can lead to a significant heating effect. As a consequence, the blue shift of the EL peak of AlInGaN–InGaN QW LEDs becomes nonobservable at room temperature.

In summary, the forward-bias voltage dependence of EL spectra of AlInGaN–InGaN QW LEDs has been studied at room temperature and low temperature. Three distinct evolution periods, the efficient screening of the built-in electric field, the band-filling effect, and heating effect, have been revealed according to the observed spectra features of device EL spectra in various bias ranges. The data provide useful information for the design and performance improvement of AlInGaN–InGaN QW LEDs.

ACKNOWLEDGMENT

S. J. Xu would like to thank V. A. L. Roy for his help in the I – V measurements of the diodes and R. X. Wang for helpful discussions. The authors would like to thank Y. Wen and X. M. Dai for participating in the variable-temperature I – V measurements.

REFERENCES

- [1] S. Nakamura, S. Pearton, and G. Fasol, *The Blue Laser Diode*. Berlin, Germany: Springer-Verlag, 2000.
- [2] K. Okamoto, A. Scherer, and Y. Kawakami, "Near-field scanning optical microscopic transient lens for carrier dynamics study in InGaN/GaN," *Appl. Phys. Lett.*, vol. 87, pp. 161104-1–161104-3, Oct. 2005.
- [3] R. Sharma, P. M. Pattison, H. Masui, R. M. Farrell, T. J. Baker, B. A. Haskell, F. Wu, S. P. DenBaars, J. S. Speck, and S. Nakamura, "Demonstration of a semipolar (10 $\bar{1}3$) InGaN/GaN green light emitting diode," *Appl. Phys. Lett.*, vol. 87, pp. 231110-1–231110-3, Dec. 2005.
- [4] B. Witzigmann, V. Laino, M. Luisier, U. T. Schwarz, G. Feicht, W. Wegscheider, K. Engl, M. Furtitsch, A. Leber, A. Lell, and V. Härle, "Microscopic analysis of optical gain in InGaN/GaN quantum wells," *Appl. Phys. Lett.*, vol. 88, pp. 021104-1–021104-3, Jan. 2006.
- [5] Y. J. Wang, S. J. Xu, Q. Li, D. G. Zhao, and H. Yang, "Band gap renormalization and carrier localization effects in InGaN/GaN quantum-wells light emitting diodes with Si doped barriers," *Appl. Phys. Lett.*, vol. 88, pp. 041903-1–041903-3, Jan. 2006.
- [6] S. J. Xu, G. Q. Li, Y. J. Wang, Y. Zhao, G. H. Chen, D. G. Zhao, J. J. Zhu, H. Yang, D. P. Yu, and J. N. Wang, "Quantum dissipation and broadening mechanisms due to electron-phonon interactions in self-formed InGaN quantum dots," *Appl. Phys. Lett.*, vol. 88, pp. 083123-1–083123-3, Feb. 2006.
- [7] L. Marona, P. Wisniewski, P. Prystawko, I. Grzegory, T. Suski, S. Porowski, P. Perlin, R. Czernecki, and M. Leszczynski, "Degradation mechanisms in InGaN laser diodes grown on bulk GaN crystals," *Appl. Phys. Lett.*, vol. 88, pp. 201111-1–201111-3, May 2006.
- [8] M. E. Aumer, S. F. LeBoeuf, S. M. Bedair, M. Smith, J. Y. Lin, and H. X. Jiang, "Effects of tensile and compressive strain on the luminescence properties of AlInGaN/InGaN quantum well structures," *Appl. Phys. Lett.*, vol. 77, pp. 821–823, Aug. 2000.
- [9] J. Zhang, J. Yang, G. Simin, M. Shatalov, M. A. Khan, M. S. Shur, and R. Gaska, "Enhanced luminescence in InGaN multiple quantum wells with quaternary AlInGaN barriers," *Appl. Phys. Lett.*, vol. 77, pp. 2668–2670, Oct. 2000.
- [10] W.-C. Lai, S.-J. Chang, M. Yokoyama, J.-K. Sheu, and J. F. Chen, "InGaN–AlInGaN multiquantum-well LEDs," *IEEE Photon. Technol. Lett.*, vol. 13, no. 6, pp. 559–561, Jun. 2001.
- [11] M. E. Aumer, S. F. LeBoeuf, B. F. Moody, S. M. Bedair, K. Nam, J. Y. Lin, and H. X. Jiang, "Effects of tensile, compressive, and zero strain on localized states in AlInGaN/InGaN quantum-well structures," *Appl. Phys. Lett.*, vol. 80, pp. 3099–3101, Apr. 2002.
- [12] D. Xiao, K. W. Kim, S. M. Bedair, and J. M. Zavada, "Design of white light-emitting diodes using InGaN/AlInGaN quantum-well structures," *Appl. Phys. Lett.*, vol. 84, pp. 672–674, Feb. 2004.
- [13] A. Hori, D. Yasunaga, A. Satake, and K. Fujiwara, "Temperature and injection current dependence of electroluminescence intensity in green and blue InGaN single-quantum-well light-emitting diodes," *J. Appl. Phys.*, vol. 93, pp. 3152–3157, Mar. 2003.
- [14] F. Rossi, G. Salviati, M. Pavesi, M. Manfredi, M. Meneghini, G. Meneghesso, E. Zannoni, and U. Strauß, "Temperature and current dependence of the optical intensity and energy shift in blue InGaN-based light-emitting diodes: Comparison between electroluminescence and cathodoluminescence," *Semicond. Sci. Technol.*, vol. 21, pp. 638–642, May 2006.
- [15] D. A. B. Miller, D. S. Chemla, T. C. Damen, A. C. Gossard, W. Wiegmann, T. H. Wood, and C. A. Burrus, "Band-edge electroabsorption in quantum well structures: The quantum-confined Stark effect," *Phys. Rev. Lett.*, vol. 53, pp. 2173–2176, Nov. 1984.
- [16] T. M. Hsu, C. Y. Lai, W.-H. Chang, C.-C. Pan, C.-C. Chuo, and J.-I. Chyi, "Electroreflectance study on the polarization field in InGaN/AlInGaN multiple quantum wells," *Appl. Phys. Lett.*, vol. 84, pp. 1114–1116, Feb. 2004.
- [17] Q. Li, S. J. Xu, M. H. Xie, S. Y. Tong, X. H. Zhang, W. Liu, and S. J. Chua, "Strong screening effect of photo-generated carriers on piezoelectric field in In_{0.13}Ga_{0.87}N/In_{0.03}Ga_{0.97}N quantum wells," *Jpn. J. Appl. Phys.*, vol. 41, pp. L1093–L13378, Oct. 2002.
- [18] Y. D. Qi, H. Liang, D. Wang, Z. D. Lu, W. Tang, and K. M. Lau, "Comparison of blue and green InGaN/GaN multiple-quantum-well light-emitting diodes grown by metalorganic vapor phase epitaxy," *Appl. Phys. Lett.*, vol. 86, pp. 101903-1–101903-3, Mar. 2005.
- [19] S. J. Xu, L. X. Zheng, S. H. Cheung, M. H. Xie, S. Y. Tong, and H. Yang, "Comparative study on the broadening of exciton luminescence linewidth due to phonon in zinc-blende and wurtzite GaN epilayers," *Appl. Phys. Lett.*, vol. 81, pp. 4389–4391, Dec. 2002.